The Effect of Faults on the Behaviour of the Earth Dam – Case Study of the Ourkiss Dam

Hassiba Beghzim (h.beghzim@univ6batna2.dz)
Batna 2 University
Toufik Karech
Batna 2 University
Tayeb Bouzid
Batna 2 University

Research Article

Keywords: Earth dam, normal fault, reverse fault, shear stress, Failure path

Posted Date: December 23rd, 2021

DOI: https://doi.org/10.21203/rs.3.rs-1123142/v1

Abstract

The analysis of the failure due to the effect of the propagation of normal and reversed faults with different angles of inclination and by sliding through the Ourkiss dam isstudied numerically. Mainly at the end of construction and at the highest water level, for this purpose the non-linear finite difference method is used considering four fault angles of inclination, activated at the center of the base of the embankment.

The results of the study show that the shear stress values increase with the increase of the vertical base displacement imposed in both conditions of the dam state, and this for both normal and overturned faults.

1. Introduction

The phenomenon of propagation of fault rupture by sliding has been studied by many authors. Bray & al [4,5] concluded that the behaviour of fault propagation is influenced by soil characteristics. It causes significant damage to the structure.Numerical simulations and physical modelling have been carried out on the phenomenon of fault fracture propagation through uniform horizontal soil layers (Bray JD & al, 1990 [5]; Bonilla, M G and Lienkaemper. JJ, 1990 [6]; Anastasopoulos. I and Gazetas.G, 2007 [1]; Lazarte C.A, 1996 [16] ; Lin. ML, & al, 2006 [17], Moosavi .SM &al 2010 [20] ; Loukidis. D& al, 2009 [18]).The study of fault propagation and its impact on the response of the underlying bedrock in the case of earth dams has been the subject of several studies. Fault displacements were first observed by Louderback(1937) [19].

This subject has been detailed by (Wieland,M& al, 2008 [29]; Sherard, J.L, Cluff, L.S, 1974 [25] Swiger, W.F, 1978 [26]; Allen, C.R, Cluff, L.S ,2000 [2]. Cheney, J.A, & al (1984) [7] analyzed fault failure in models of silt embankments using centrifugation tests.In order to study the influence of material properties, geometry and kinematic conditions on the response of the saturated clay backfill due to a Lazarte fault, 1996 [16] carried out a physical model test with experimental studies and 3D numerical analyses. Mejia &coll (2005) [21] numerically studied the combined effects of earthquakes and fault displacement of the foundation of the Aviemore Dam in New Zetland. Solhmirzaei& al (2012) [27] numerically model the propagation of the failure of an active dipping fault through clayey soil. Soroush& al (2015) [28] numerically studied two homogeneous and zoned embankment dams when faults occur in their underlying bedrock under steady-state infiltration conditions.Khoshini& al (2014) [15] and MortazaviZanjani& al (2016) [22] carried out finite element analyses on zoned homogeneous earth dams in an attempt to define fault propagation and consequently the stability of the Ejlali dam & al (2015) [9] analysed the propagation paths of the fault rupture through a zoned embankment dam. Hazeghian&Soroush (2015) [11],(2017) [12]have shown that the inclinations of fault failures are in agreement with Roscoe's theory (Roscoe, 1970).Hazeghian & Soroush (2018) [13] have carried out numerical parametric analyses examining the effect of soil surface geometry on the propagation of slip

faults through granular soil. Finally, Eeleni& al (2019) [10] focused their work on the effects of normal fault propagation on a motorway embankment based on a single-layer soil.

2. Presentation Of The Ourkiss Dam

The Ourkiss Dam is an embankment dam built with clayey materials and alluvium with a watertight geomembrane screen on the upstream face of the dike and on the sides of the dam. It is located 14 km south of the town of Ain Fakroune, downstream of the confluence of Wadi El Kebir and Ourkiss, in the wilaya of Oum el Bouaghi. The height of the dam is 40.60 m, the crest being 407 m long and 8 m wide at the height of 954.50 m NGA (Algerian General Levelling). The reservoir has a normal elevation of 951.60 m NGA with a total storage volume of 69.1 × 106 m3. The slope inclination upstream is 1:3 while the slope inclination downstream is 1:2.5 (Fig. 1).

The area of the dam and the sides of the reservoir are made up of much karstified dolomitic, calcareous and dolomitic limestone hard rocks. Mostly subvertical faults are observed, up to several meters wide with an average extent in the East-West direction. Movements up to several tens of meters have been observed along these faults.

The most pronounced structural form in the area of investigation is certainly the fault zone (red fault) of about 5 m wide, along which the rock (dolomite) is very broken and later degraded to the waffle and filled with clay. It extends along the whole area of the map; it cuts the initial part of the gallery on the right flank and the drainage channel (Fig. 1). For the modeling of the dam we take profile 8 whose dimensions are shown in Fig. 1.

3. Problem Definition And Model Description

3.1) Geometry and boundary conditions

The numerical analysis of the propagation of the active fault fracture through the Ourkiss dam filled and at the end of construction was studied using FLAC 2D [14] in plane deformation mode with a Mohr-Coulomb elastoplastic criterion. The research focuses mainly on the quasi-static dislocation and normal and reverse propagation of the fault with various submergence angles α (30°-45°-60°-75°), with the fault tip located in the center of the overlying embankment at the base of the dam.

To simulate the movement of the fault, a displacement with angles of inclination α is applied to the left (upstream) part while the right part is fixed [28] figure 2.

3.2) Loading application:

The basic vertical displacement (h) necessary for the propagation of the fracture through the structure for uniform horizontal layers of non-cohesive material is 2 to 6% of the height of the overlying layer is

imposed according to [5,8, 18]. Bray & al [5] base displacements of 10 to 16% of the height are required for horizontal layers of saturated clay materials [23].

However, the materials commonly used in backfill are stiffer than saturated clay materials. Preliminary analyses in this study reveal that smaller base displacements are sufficient for the development of a fracture across the trapezoidal geometry of the embankments [23]. Mortazavi Zanjani and Soroush (2014, 2016) suggested a vertical base displacement of 2% and 4% of the size of the dam for normal (NF) and reverse (RF) faults respectively in order for the failure to reach the ground surface. On the basis of these studies, we have chosen equivalent vertical displacements as shown in Table 1.

Table 1: Choice of basic vertical displacement "h".

	Value of vertical base displacement h and type of fault	
	Normal fault (NF)	Revers fault (RF)
The fault point is located in the backfill center	2% H = 0.68 m 2.94 % H =1m 4.41 % H =1.5m	4% H = 1.36 m 2.94 % H =1m 4.41 H =1.5m

3.3) Geotechnical parameters.

Presentation of the geotechnical parameters of different zones of the Ourkiss Dam.

Table 2: Geotechnical parameters of the model.

Geotechnical Horizon	Foundation	Alluvial Materials	Clay
Volume weight:γ (kN/m3)	22.6	19.00	19.30
Friction angle : ϕ (°)	40°	30 °	20°
Cohesion : C (kPa)	00.00	5.00	10,0
deformabilityModulus:E (barre)	120.00	60.00	50.00
Poisson's coefficient : V	0,25	0,4	0,33
Behaviour law	MC	MC	MC

NB/ MC: Mohr-Coulomb Law of Behavior

4. Presentation And Discussion Of Results

4.1.1) End of construction case (EOC) h=1m normal fault (NF).

4.1.2) Higher water level case(HWL) h=1m normal fault (NF).

4.1.3) End of construction case (EOC) h=0.68m normal fault (NF).

4.1.4) Higher water level case (HWL) h=0.68m normal fault (NF)

4.1.5) End of construction case (EOC) h=1.5m normal fault (NF)

4.1.6) Higher water level case (HWL) h=1.5m normal fault (NF)

According to figures "3-4-5-6-7-8", it can be said that the general fracture profiles for normal faults with the inclination α= 30◦, 45◦ for the Ourkiss dam are similar to those found by

M. Hazeghian & al (2018) [13] (Figure 10), both for the state at the end of construction and that of the highest water level.

A primary crack first occurs downstream, then a secondary asymmetric fault fracture develops upstream. Another comparison with similar works but for an earth dam zoned for a normal fault α= 45° by a M. Zanjani& al 2016 [22] (Figure 3) was made with the Ourkiss dam study.

On the basis of the general fracture patterns that have been developed for normal faults, with the inclination α = 60◦, 75◦ (figures "3-4-5-6-7-8") we can describe this state of facts as follows : A primary fracture develops upstream, then a secondary fracture evolves downstream, at the end of the construction for the basic vertical displacement h=1.5m, h=1m and h=0.68m.

On the other hand, for the upper level normal fault state (α = 75◦), only a primary fracture develops on the downstream side for the basic vertical displacements h=1.5m, h=1m and h=0.68m. But for α = 60°, a primary fracture is formed upstream, with a secondary fracture developing downstream. These results are consistent with the results obtained by M. Hazeghian& al (2018) [13] figure 10.

4.2) Diagrams of fault ruptures reversed fault cases (RF):

4.2.1) End of construction case (EOC) h=1m reverse fault (RF)

4.2.2) Higher water level case (HWL) h=1m overturn fault (RF)

4.2.3) End of construction case (EOC) h=1.36m reverse fault (RF)

4.2.4)Higher water level caseHWL case h=1.36m reverse fault (RF)

4.2.5) End of construction case (EOC) h=1.5m reverse fault (RF)

4.2.5) Higher water level caseHWL case h=1.5m reverse fault (RF)

With respect to the reverse fault with α = 30°, the summary results presented in Figures 10-11-12-13-14-15 show that there are primary (P) and secondary (S) failures across the dam. They diverge downstream for the two conditions, end of construction (EOC) and higher level of water(HLW), and this regardless of the value of the vertical displacement of the base h, in comparison with the distribution of the fault lines found by Zanjani and Soroush (2013) [23] we see that they are close to the surface and shallow in a

trapezoidal geometry Figure 16. While for α = 45° the figures (10-11-12-13-14-15) show that the rupture line in our case propagates towards the crest and the downstream side. On the other hand, the break line in the case of the MortazaviZanjani M, Soroush A, Khoshini M [20] study propagates out of the core towards the upstream and downstream sides at the base of the dam and this is due to the effect of the core stiffness.

About the reverse fault α = 60 ° and α = 75 °, the figures (10-11-12-13-14-15) show that the primary ruptures (P) through the Ourkiss dam, deviate from the fault projection lines upstream, for both conditions (EOC) and (HWL). These results are consistent with the work of Zanjani and Soroush (2013) [23]. For the case where h=1.5m, we find that under both EOC and HLW conditions and for α = 60°, the P ruptures across the dam deviate from the fault projection lines towards the downstream side.

5. Comparison Of Shear Stress Increments

In order to demonstrate the importance of the distribution of shear stress increments (SSI) as a function of the state of the two dam conditions (EOC and HWL) and the type of fault (RF and NF), a graphical presentation is shown in the figure below.

According to Figure 17 (a and b) (h=0.68 m and h=1.36 m), it can be seen that in the case of the presence of a reverse fault, the increases in shear stress are greater than those of a normal fault. For the case when α=30° representing the HLW angle, the increases in shear stress for a normal fault become significant.

It appears from Figure 18 (a and b) (h=1. 5m) that at the end of construction (EOC) the shear stress increments for a normal fault are greater than for an reverse fault for α=45° and α=60° as opposed to α=30° and α=75°. It should also be noted that the shear stress increments for a reverse fault become important for the condition of the dam in case of higher water level. In the case of the presence of a normal fault the shear stress increments are more important than in the case of a reverse fault, independently of the values of the angles of inclination α.

According to Figure 19 (a and b) (h=1m) it can be seen that for both dam conditions, end of construction and higher water level, the shear stress increases for a normal fault are greater than for a reverse fault and these values are devoid with increasing angles of inclination α.

6. Conclusions

Numerical analyses of the propagation of normal and reversed shear cracks in the Ourkiss Dam in the finite element state (EOC) and the upper water level state (HWL) were performed. Four angles of inclination were applied to the center of the base of the dam, resulting in the following remarks and conclusions:

- The shear stress values increase with the increase of the vertical base displacement for both conditions (EOC and HWL) and this for both the normal fault and the reversed fault.
- The core stiffness has an influence on the direction of crack propagation in the fault.
- In the case of a reversed fault, the shear stresses take higher values compared to a normal fault and this for both dam conditions (EOC and HWL), independently of the inclination values α under the effect of the two basic vertical displacement values 4% and 2% of the dam size for the normal (NF) and reversed (RF) faults respectively.
- For the basic vertical displacement values of 4.41% and 2.94% of the dam height, the shear stresses for a normal fault are higher than for a reversed fault.
- Different failure modes can develop inside the Ourkiss dam, depending on the type of fault (normal or reversed) and the angle of the fault.

References

[1] Anastasopoulos I, Gazetas G, Bransby MF, Davies MCR, Nahas A EI 'Fault rupture propagation through sand: finite-element analysis and validation throughcentrifuge experiments'. J Geotech GeoenvironEng 2007;133(8):943–58.

[2] Allen C.R, CluffL. S. 'Active faults in dam foundations': an update. In: Proceedings of 12th world conference on earthquake engineering, Auckland, New Zealand; 2000.

[3] Bray JD, Seed.R, CluffL, Seed B. 'Earthquake fault rupture propagation through soil'. JGeotechEng, ASCE1994; 120 (3): 54361.https://doi.org/10.1061/(ASCE)07339410(1994)120:3

(543).

[4] Bray J.D. 'Developing mitigation measures for the hazards associated with earthquake surface fault rupture'. Works hopon seismic fault-induced failures–possible remedies for damage to urban facilities. Research Project 2000Grant-in-Aidfor Scientific Research (No.12355020).Tokyo,Japan; 2001January11-12,pp.55-79 [Invited Paper].

[5] Bray J.D, Seed R.B, Seed H.B. 'The effect of tectonic movements on stresses and deformations in earth embankments'. Earthquake Engineering Research Center, University of California at Berkeley, Report no. UCB/EERC-90/13; 1990.

[6] Bonilla M.G, Lienkaemper J.J. 'Visibility of fault strands in exploratory trench sand timing of rupture events'. Geology 1990; 18:153–6.

[7] Cheney J.A, Shen CK, Ghorayeb F. 'Fault Movement: Its Potential Damage to Embankment Dams'. In: Proceedings of 8th world conference on earthquake engineering. San Francisco, California; 1984. p. 341–347.

[8] Cole D.A. J.r., Lade P.V, 'Influence Zones in Alluvium Over DipSlipFaults', Journal of Geotechnical Engineering Division, ASCE, 1984, 110 (5), 599-615.

[9] Ejlali.Z, Vafaeian.M, Eslamihaghighat .A, Fadaee.M ' Fault rupture propagationthrough zoned embankment dams'. Proceedings of the 7th international conferenceon seismology and earthquake engineering; 2015 may 18-21, Tehran, Iran.

[10] Eleni. P∗, Nikolaos .K ' Exploring the interplay between normal fault rupture and ahighway embankment founded on a single-layered soil:Mapping and quantification of damage'DepartmentofCivilEngineering,DemocritusUniversityofThrace,BuildingB-ampusXanthi-Kimmeria,Xanthi,Greece

[11] Hazeghian, M., &Soroush, A. (2015). 'DEM simulation of reverse faulting through sands with the aid of GPU computing'. Computers and Geotechnics, 66, 253–263.

[12] Hazeghian, M., &Soroush, A. (2017). 'Numerical modeling of dip-slip faulting through granular soils using DEM'. Soil Dynamics and Earthquake Engineering, 97, 155–171

[13] Hazeghian M, Soroush A. 'DEM simulation to study the effects of the ground surface

geometry on dip-slip faulting through granular soils'. Eur J of Environ and CivEng2018:1–19. https://doi.org/10.1080/19648189.2018.1428225. Taylor & Francis.

[14] Itasca FLAC-fast langrangi ananalysis of continua. Minneapolis, MN: Itasca Consulting Group; 2011.Version7.0.

[15] Khoshini.M, Soroush.A, Mortazavi Zanjani.M.'Stability of embankment dams subjected to faulting'. Proceedings of the 2ndeuropean conference on earthquake engineering and seismology; 2014 august 25-29, Istanbul, Turkey.

[16] Lazarte CA. 'The response of earth structures to surface fault rupture' (PhDDissertation).Berkeley: University Of California; 1996.

[17] Lin .ML, Chung .CF, Jeng.FS 'Deformation of overburden soil induced by thrustfault slip'. EngGeol 2006; 88:70–89.

[18] Loukidis.D, Bouckovalas.GD, Papadimitriou, AG. 'Analysis of Fault RupturePropagation Through Uniform Soil Cover'. Soil DynEarthqEng 2009;29: 1389–404.

[19] Louderback.GD. 'Characteristics of active faults in the central coast ranges ofCalifornia, with application to the safety of dams'. SeismolSoc Am Bull 1937;27(1):1–27.

[20] Moosavi.SM, Jafari.MK, Kamalian. M, Shafiee.A ' Experimental investigation ofreverse fault rupture–rigid shallow foundation interaction'. Int J CivEng 2010;8(2):85–98.

[21] Mejia .L, Walker .J, Gillon. M. ‘Seismic evaluation of dam on active surface fault’. In: Proceedings of waterpower XIV conference. Austin, Texas; 2005

[22] MortazaviZanjani . M, Soroush. A, Khoshini. M. ‘Two-dimensional numerical modeling of fault rupture propagation through earth dams under steady state seepage’. SoilDynamEarthqEng2016;88:60–71.

[23] MortazaviZanjani, M., &Soroush, A. (2013). ‘Numerical modeling of reverse fault rupture propagation through clay embankments’. International Journal of Civil Engineering, 11, 122–132

[24] Ministry of water resources national agency of dams and transfers document monographpiece N ° 1: textual part of ourkiss dam (wilaya of Oum EL Boughi)

[25] Sherard .JL, Cluff.LS, Allen CR. ‘Potentially active faults in dam foundations’.Geotechnique 1974;24:367–427.

[26] Swiger.WF. ‘Specialty session on design for fault displacement’, ASCE specialty conference, earthquake engineering and soil dynamics; 1978.

[27] Solhmirzaei.R, Soroush.A, MortazaviZanjani.M.’ Numerical analysis of effects of fault rupture on overlying soil structures’. Proceedings of the 1st internationalconference on dams and hydropower; 2012 february 8-9, tehran, Iran.

[28] Soroush.A, Khoshini.M, MortazaviZanjani.M ’Faulting effects on stability of embankmentdams’. Proceedings of the 15th asian regional conference on soil mechanicsand geotechnical engineering; 2015 november 9-13, fukuoka, Japan.doi:10.3208/jgssp.IRN7.

[29] Wieland .M, Brenner .RP, Bozovic . A. ‘Potentially active faults in the foundation of large dams part I: Vulnerability of dams to seismic movements in dam foundation’. In: Proceedings of the fourteenth international conference on earthquake engineering, Beijing, China; 2008

Figures

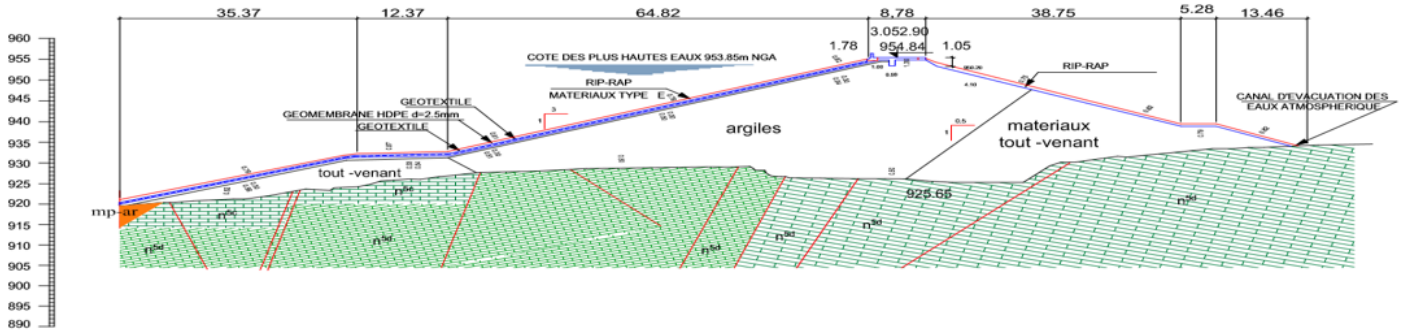

Figure 1

profile 8 of the Ourkiss dam

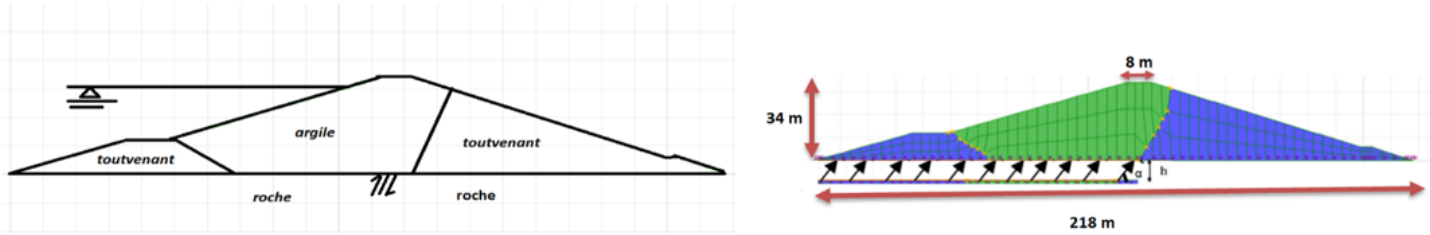

Figure 2

The tip of the fault is located in the center of the overlying embankment

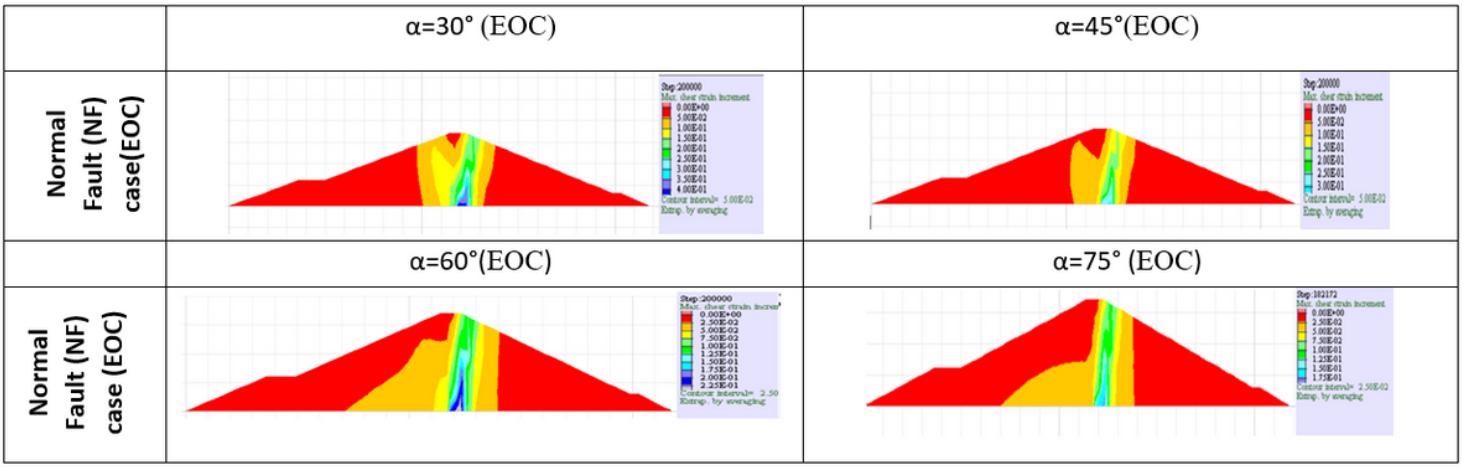

Figure 3

rupture diagrams of the faults developed in the Ourkiss dam in terms of maximum shear deformation contours at the end of construction (EOC) h=1m (NF)

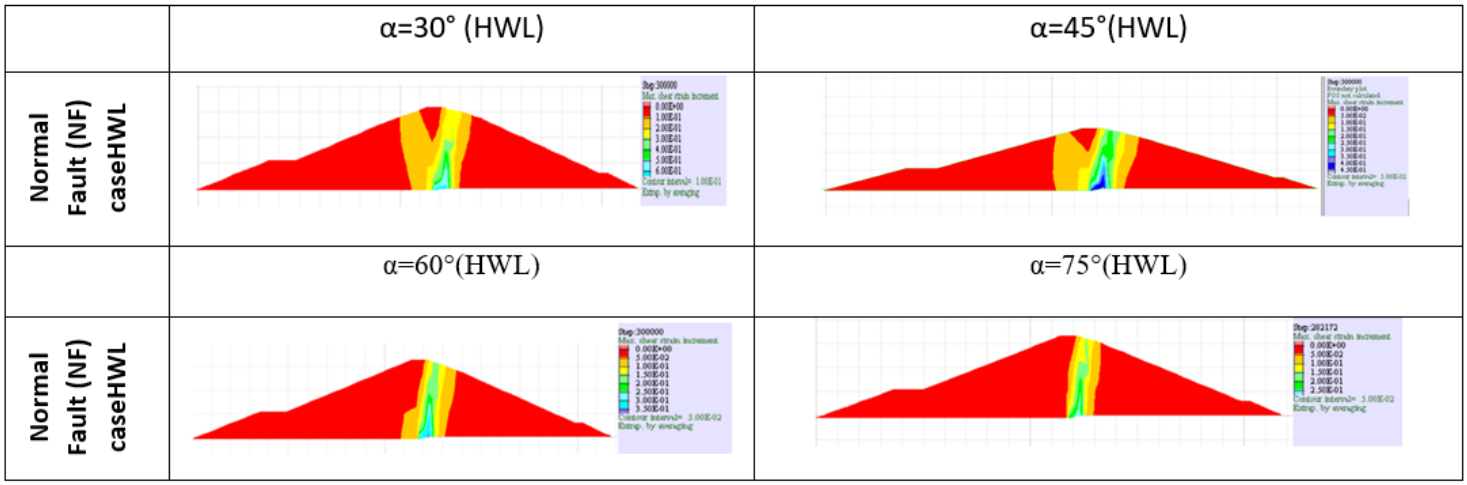

Figure 4

rupture diagrams of the faults developed in the Ourkiss dam in terms of the maximum shear deformation contours in case of higher water level(HWL) h=1m (NF)

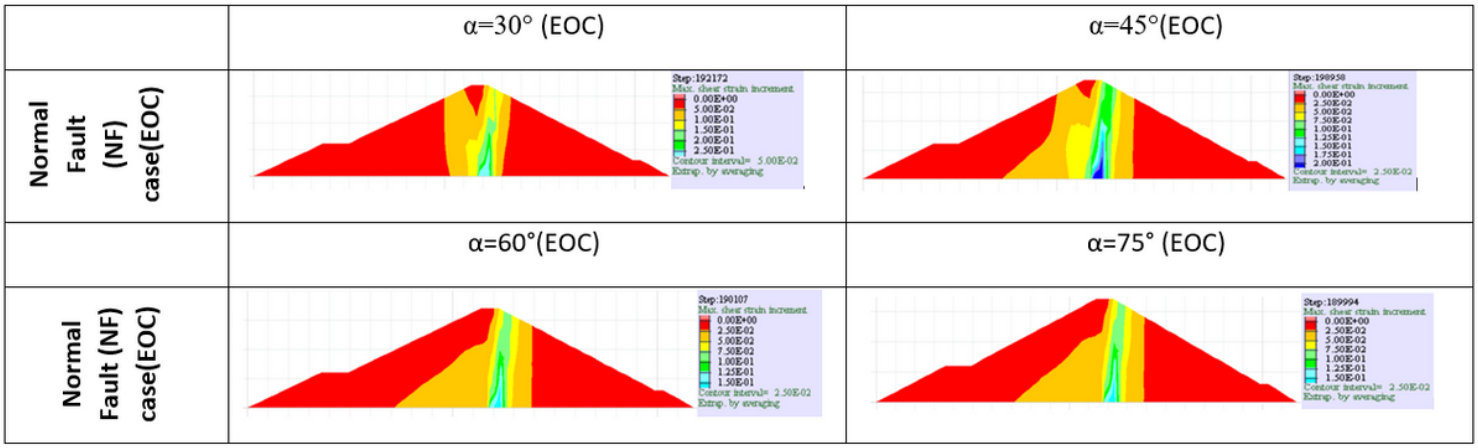

Figure 5

rupture diagrams of the faults developed in the Ourkiss dam in terms of maximum shear deformation contours at the end of construction (EOC) h=0.68 m (NF)

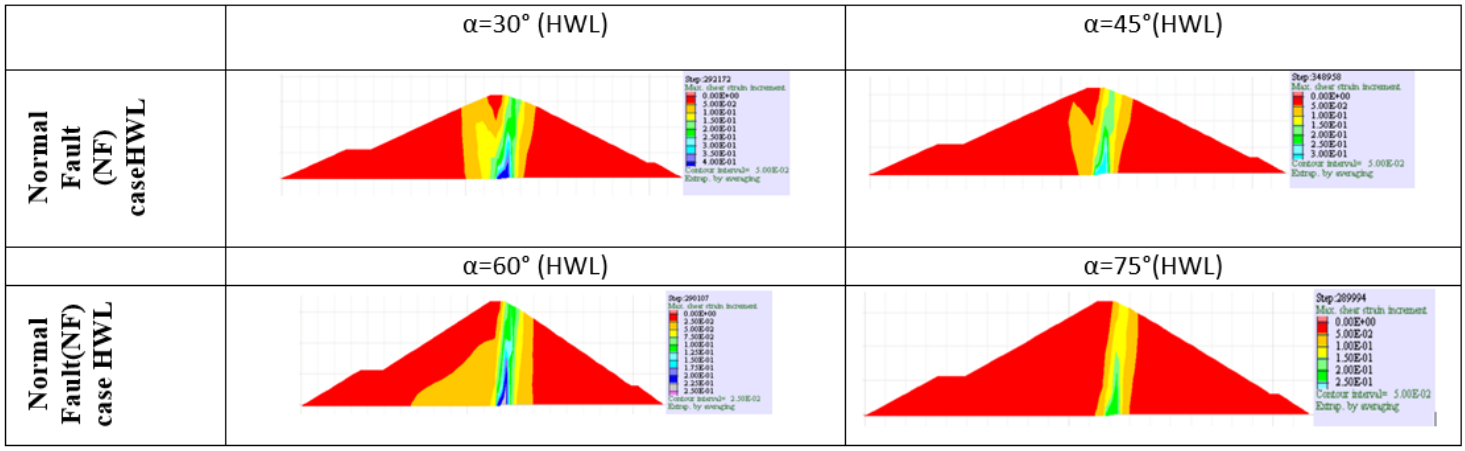

Figure 6

rupture diagrams of the faults developed in the Ourkiss dam in terms of maximum shear deformation contours in case of higher water level(HWL)h=1.5m (NF)

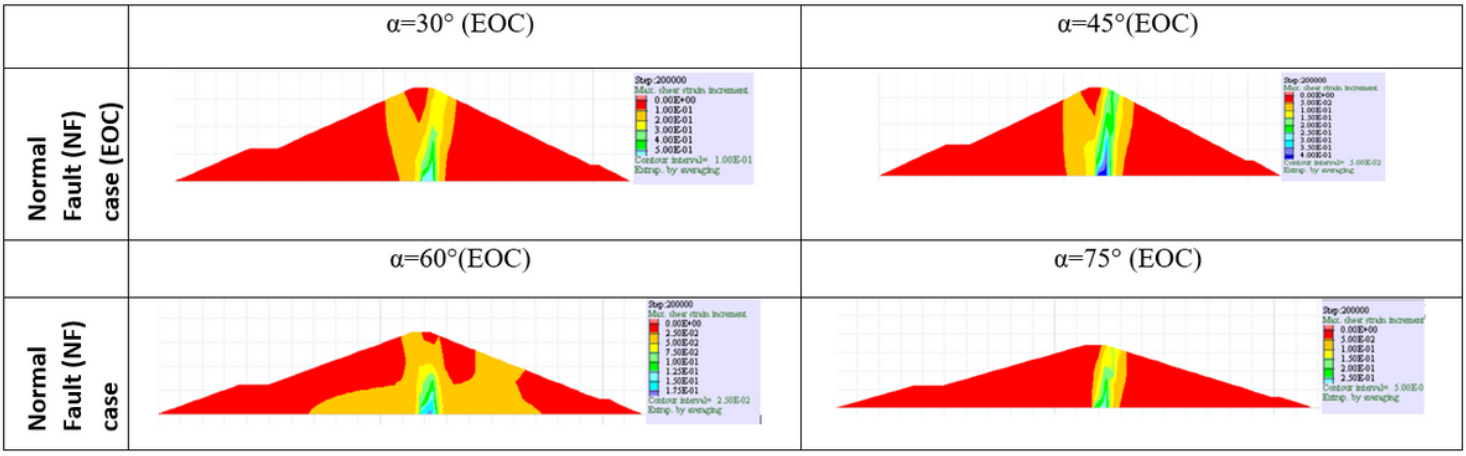

Figure 7

rupture diagrams of the faults developed in the Ourkiss dam in terms of maximum shear deformation contours at the end of construction (EOC) h=1.5 m (NF)

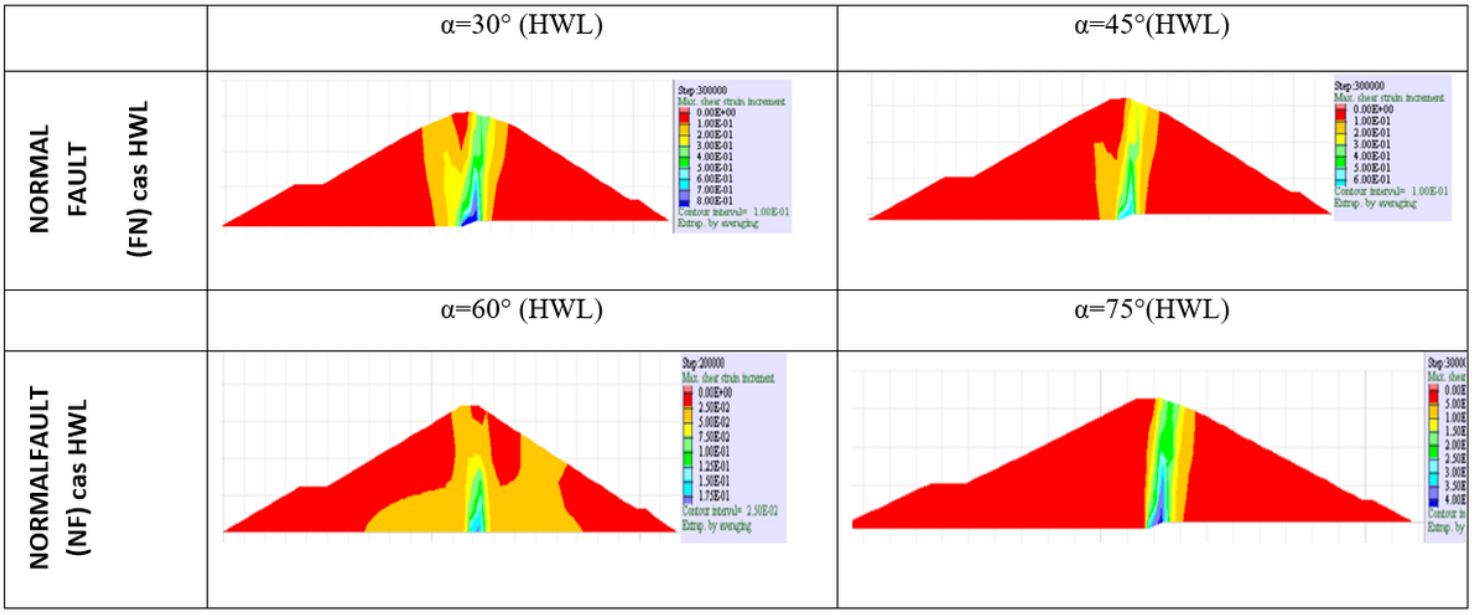

Figure 8

Fault fracture patterns of the faults developed in the Ourkiss Dam in terms of maximum shear deformation contoursin case of higher water level(HWL)case h=1.5m (NF)

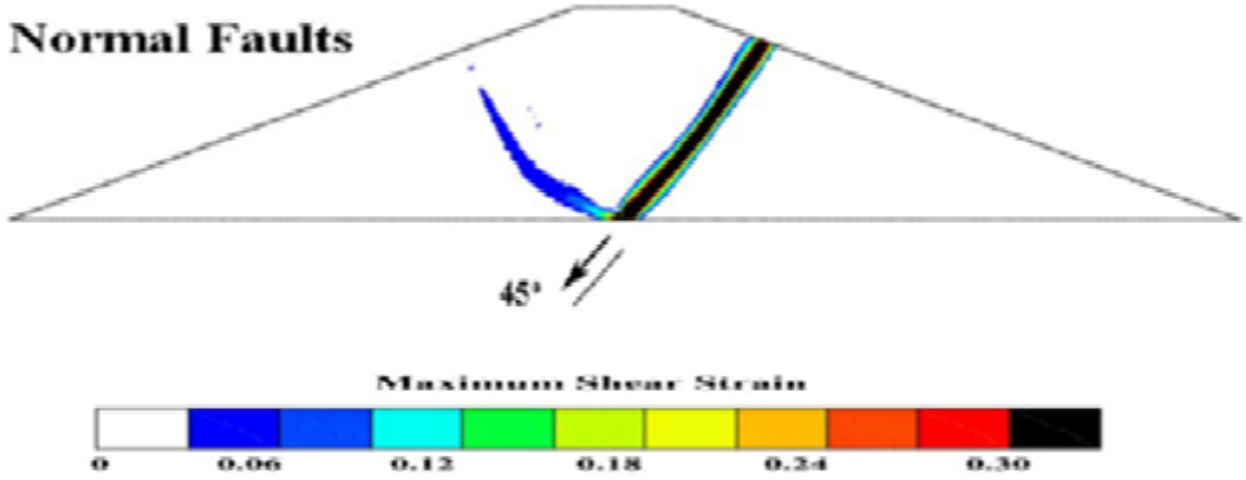

Figure 9

Rupture propagation of the normal fault for α= 45 ° activated at the center of the base of the zoned dam (Mortazavi Zanjani. M, Soroush A, Khoshini.M [22])

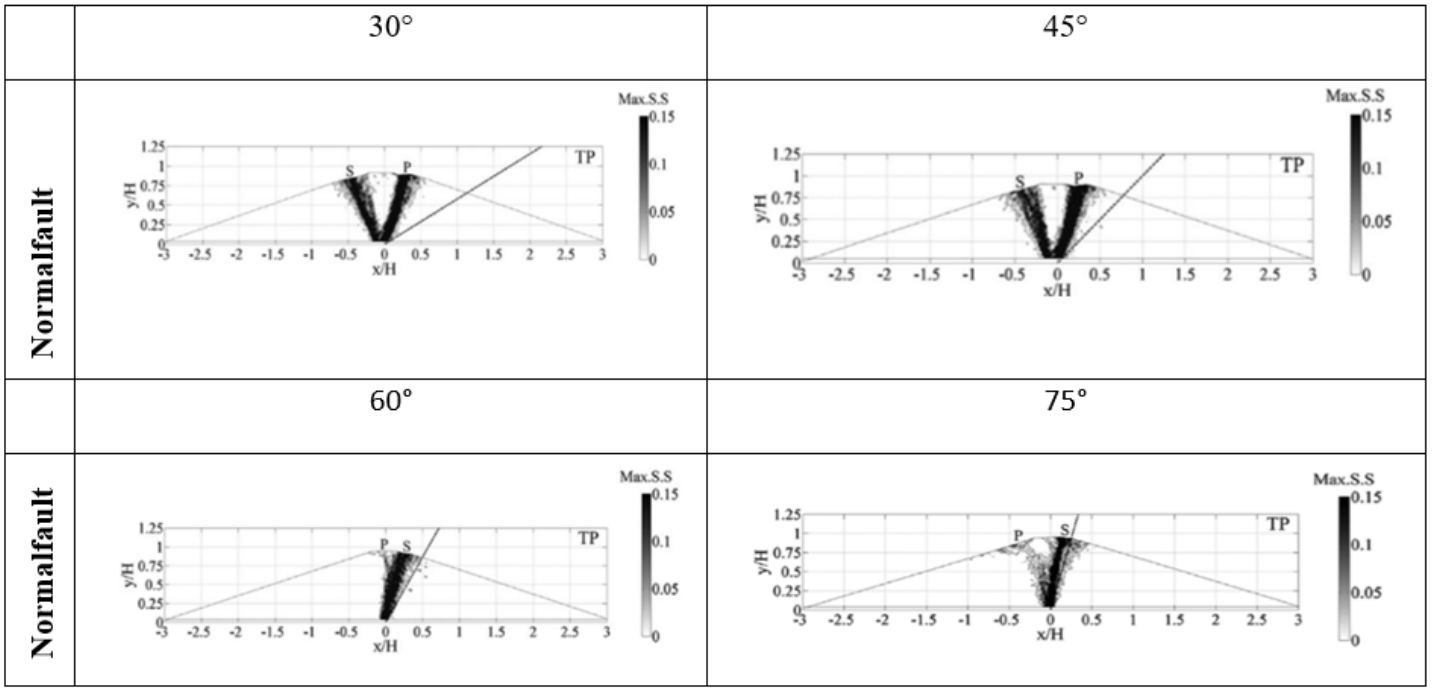

Figure 10

Fault fracture patterns of the faults developed in the embankment in terms of maximum shear deformation (normal faults) (Hazeghian& al (2018) [13]).

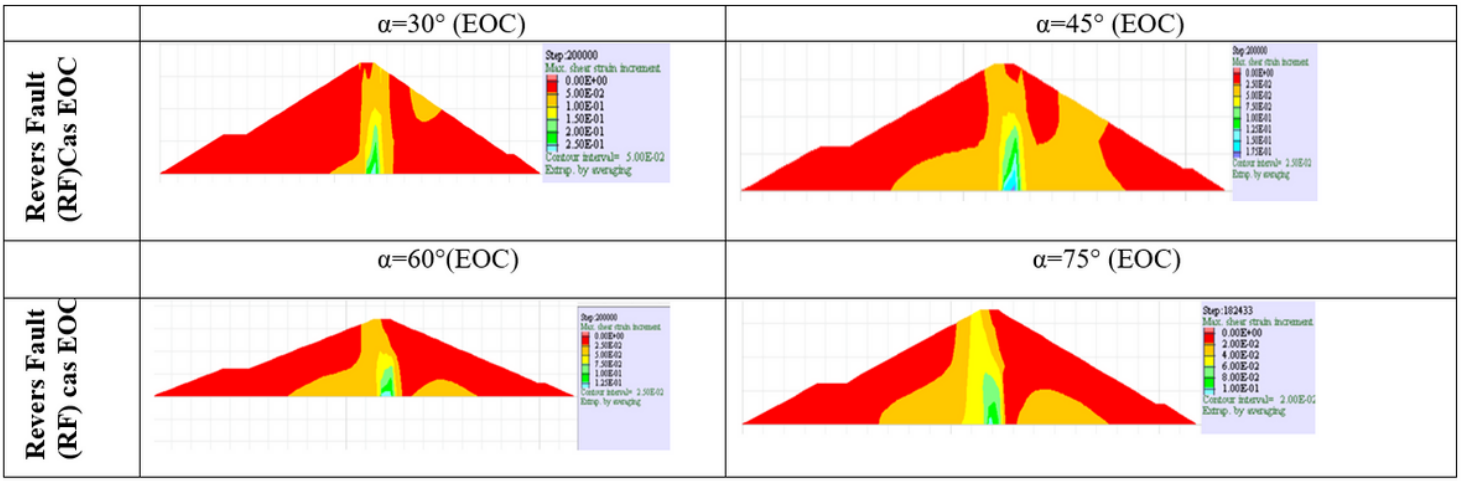

Figure 11

Fault rupture diagrams of the faults developed in the Ourkiss dam in terms of maximum shear deformation contours at the end of construction (EOC) h=1m (RF)

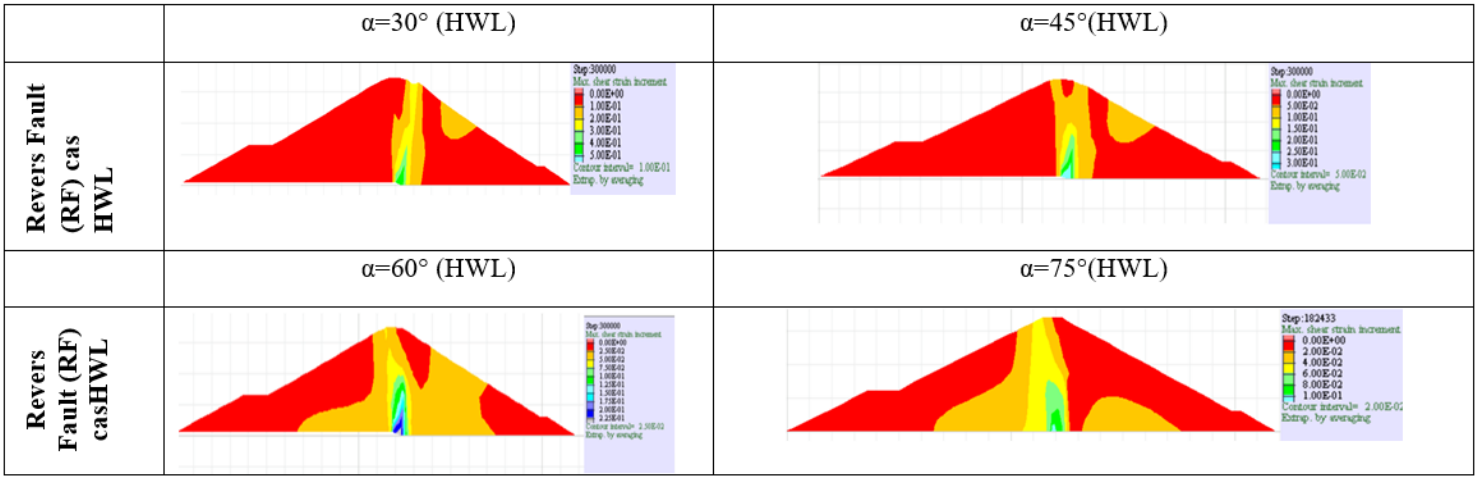

Figure 12

Fault rupture diagrams of the faults developed in the Ourkiss dam in terms of the maximum shear deformation contours in caseof higher water level (HWL) h=1m (RF)

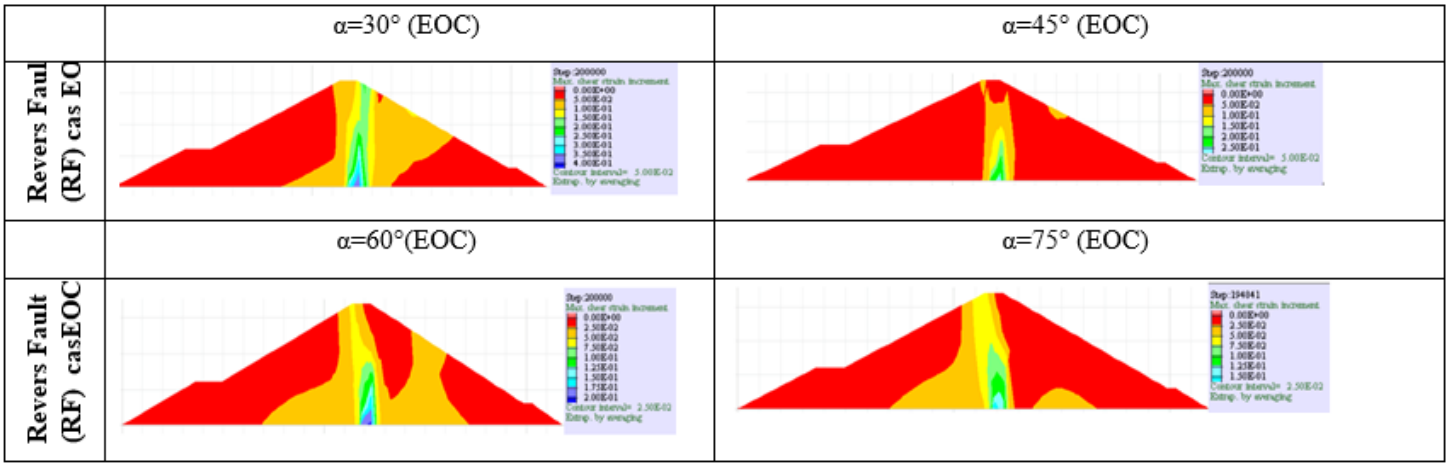

Figure 13

Fault rupture diagrams of the faults developed in the Ourkiss dam in terms of maximum shear deformation contours at the end of construction (EOC) h=1.36 m (RF)

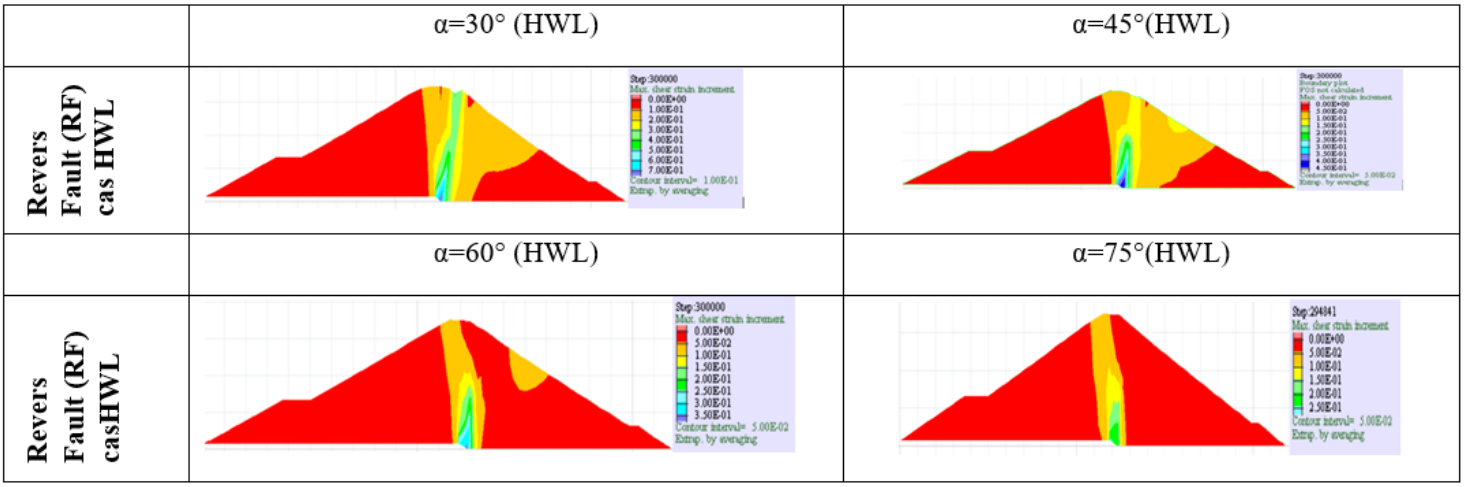

Figure 14

Fault rupture diagrams of the faults developed in the Ourkiss dam in terms of

maximum shear deformation contours in case of higher water level (HWL) h=1.36m (RF)

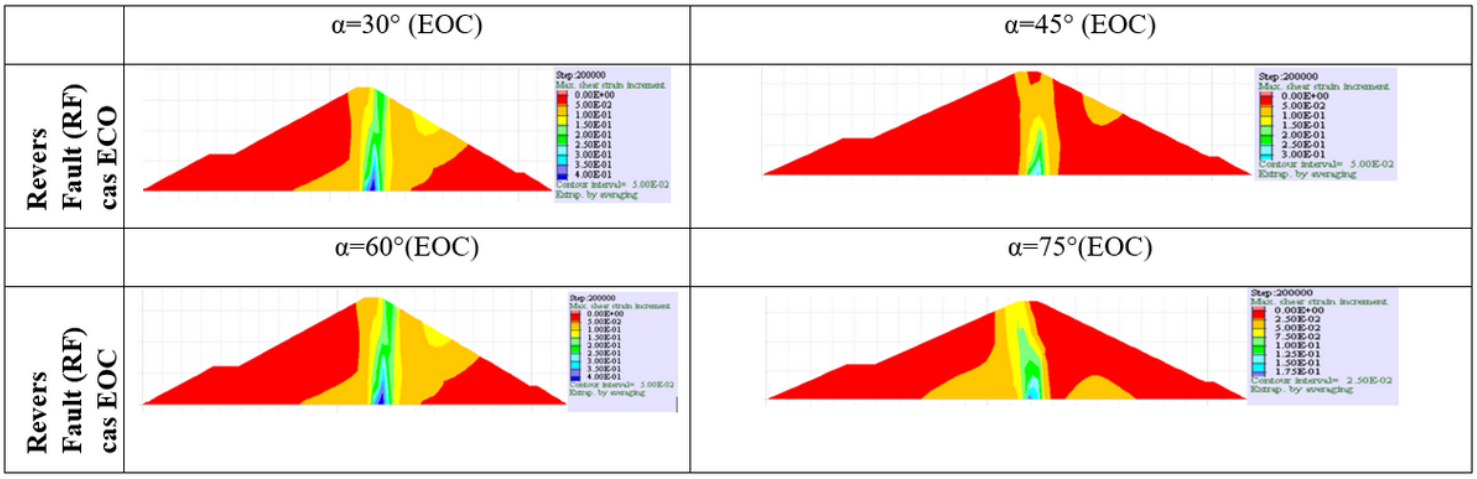

Figure 15

Fault rupture diagrams of the faults developed in the Ourkiss dam in terms of maximum shear deformation contours at the end of construction (EOC) h=1.5m (RF)

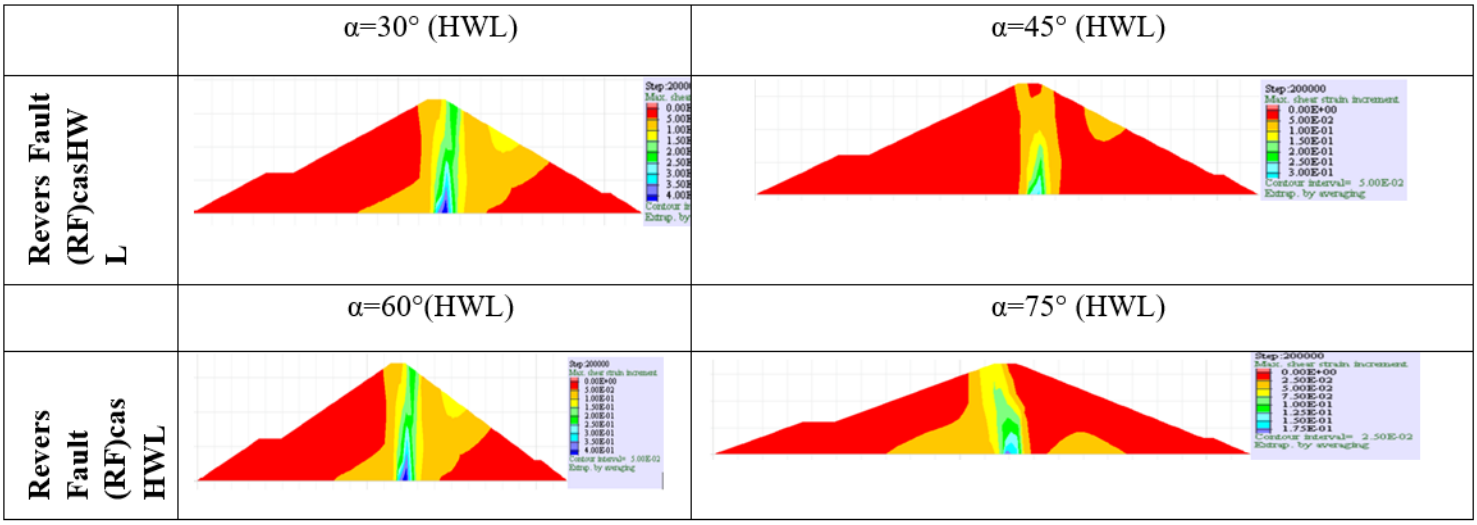

Figure 16

Fault rupture diagrams of the faults developed in the Ourkiss dam in terms of

maximum shear deformation contours in case of higher water level (HWL)h=1.5m (RF)

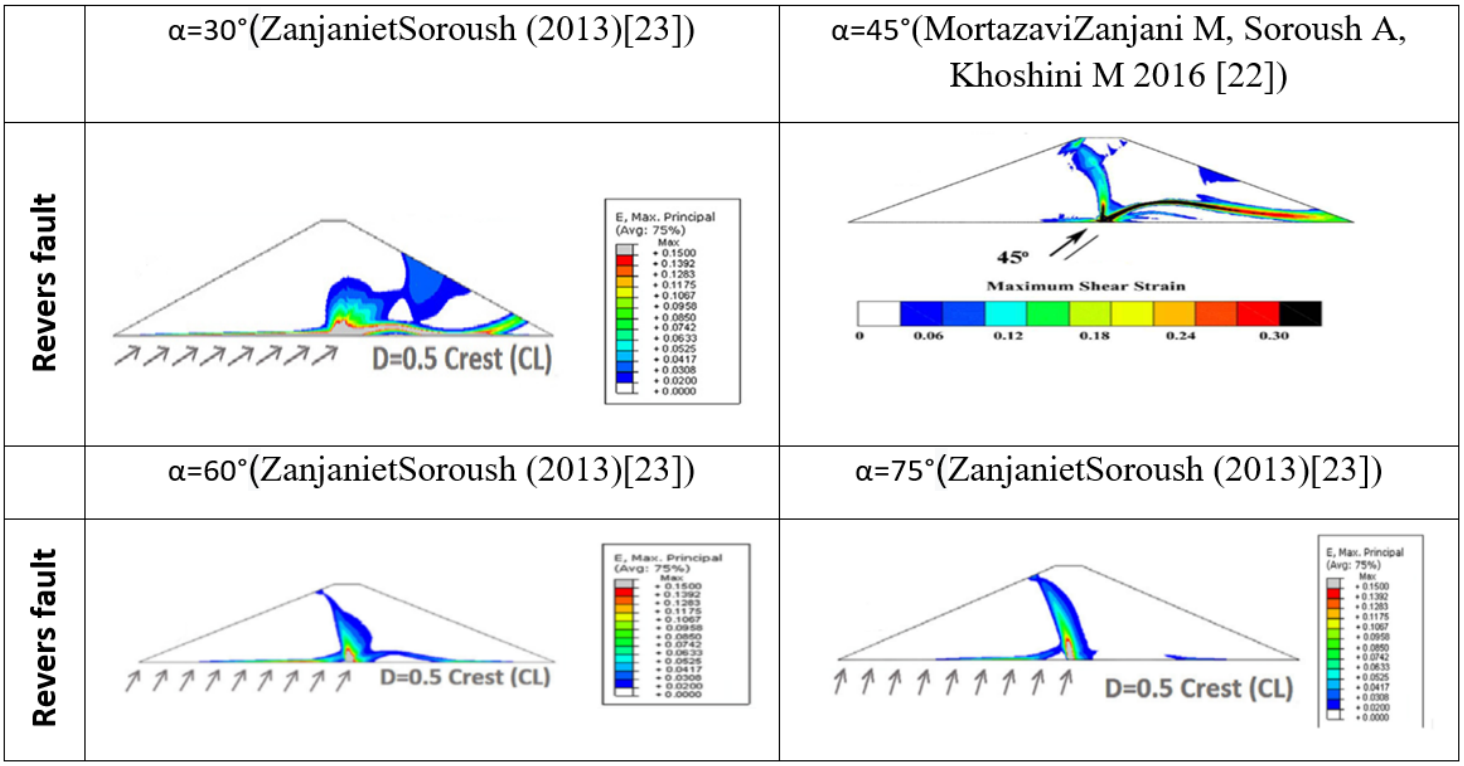

Figure 17

Propagation of the reverse fault rupture in a clay embankment)[23] and a zoned dam)[22].

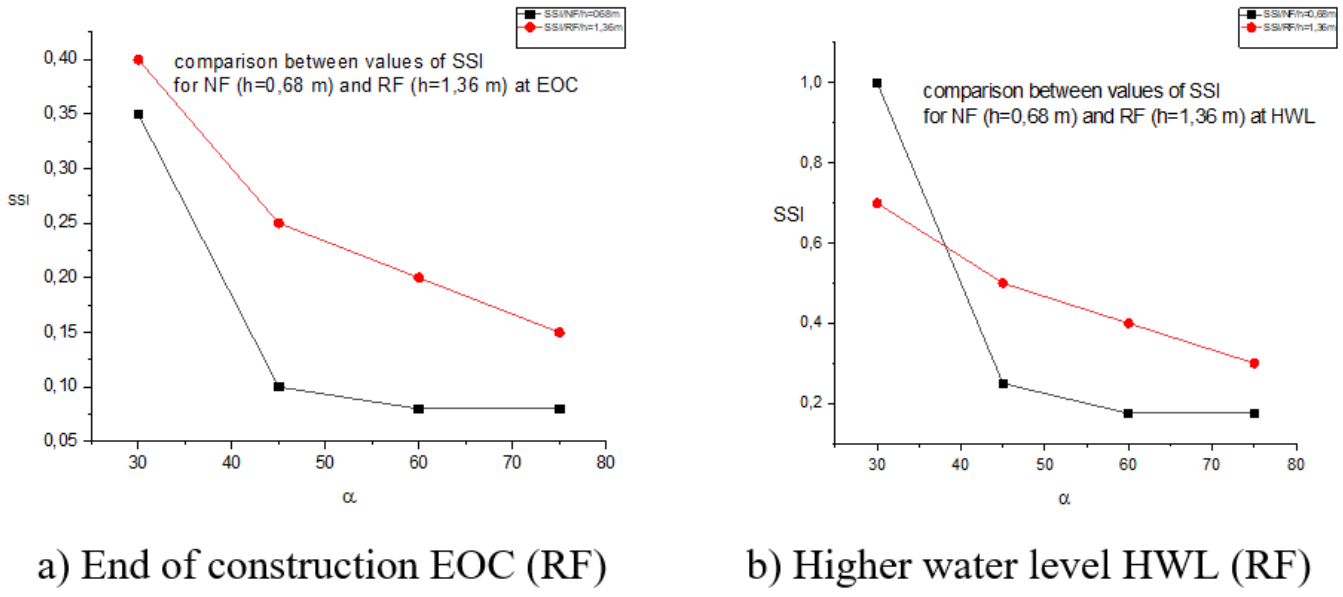

a) End of construction EOC (RF)

b) Higher water level HWL (RF)

Figure 18

Variation of shear stress increments (SSI) as a function of α and h (h=1.36m and h=0.68m)

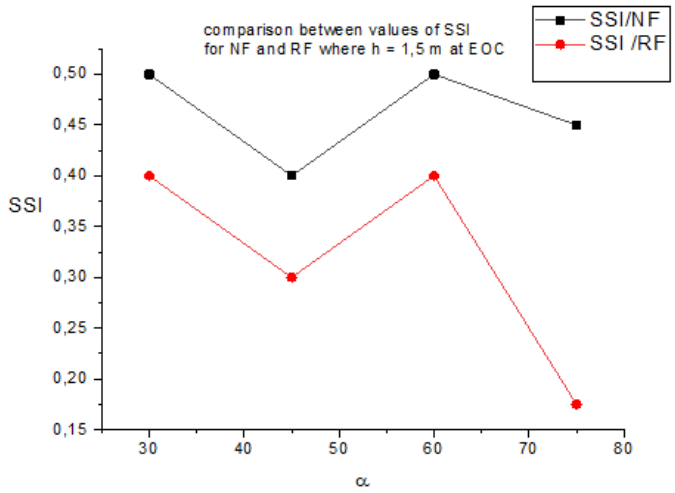

a) End of construction EOC (RF)

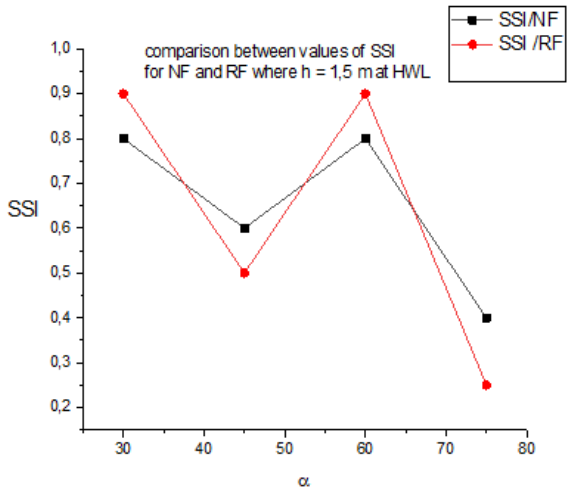

b) Higher water level HWL (RF)

Figure 19

Variation of shear stress increments (SSI) as a function of α and h (h=1.5)

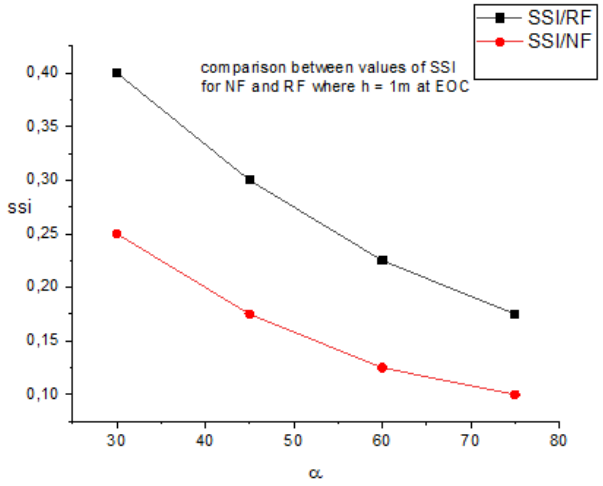

a) End of construction EOC (RF)

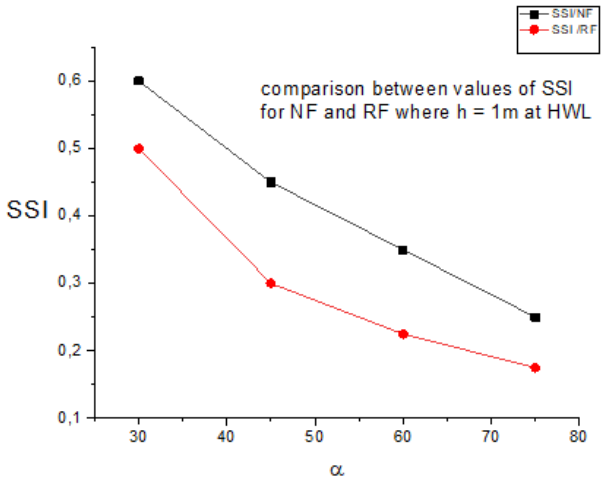

b) Higher water level HWL (RF)

Figure 20

Variation of shear stress increments (SSI) as a function of α and h (h=1 m)